Gravitational Trap for Space Debris in GEO

Vladimir S. Aslanov[1]
Samara National Research University, 443086 Samara, Russia

Nomenclature

m	=	mass of the space debris (target), kg
m_1	=	mass of the Earth, $5.9742 \cdot 10^{24}$ kg
m_2	=	mass of the orbital collector (chaser), kg
m_3	=	mass of the Moon, $6.6710 \cdot 10^{11}$ kg
L_1, L_2	=	the Lagrangian points
μ	=	$m_2 / m_1 + m_2$
μ_m	=	$m_3 / m_1 + m_3$
r	=	the distance between the Earth and the orbital collector, m
R	=	the distance between the Earth and the Moon, $384.4 \cdot 10^6$, m
G	=	the Newtonian gravitational constant, $6.67428 \cdot 10^{-11}$, m^3 s^{-2}kg^{-1}
n	=	the mean motion of the chaser, s^{-1}
ω	=	the mean motion of the Moon, s^{-1}
α, ρ	=	the polar coordinates the Cartesian coordinates M_2XY

I. Introduction

There are more than 30.000 large objects in orbit around the Earth. Only 5% of these are active spacecraft, 17% are nonfunctional spacecraft, 13% are orbital stages of rockets and the remaining percentage includes fragments [1]. Space debris is a growing concern for both Leo Earth Orbit (LEO) and Geosynchronous Orbit (GEO) regimes [2]. The collisions of large space debris with other debris can significantly increase the number of small debris on the Earth orbit. The debris cascade effect described by Kessler has begun to occur [3]. Several orbits can be dangerous for new missions therefore large debris should be removed. The choice of the active debris removal technique depends on properties of space debris. Recently several active debris removal methods have been developed [4]–[7]. There are three types of the connection between a space tug and a space debris: flexible connection, rigid connection and distant interaction. The act of docking onto such large and tumbling space objects is very challenging, and as a result novel touchless debris removal or despinning solutions are being explored. The ion-shepherd method uses the ion engine exhaust to push and/or despin a satellite [7-8], while the laser ablation method uses the debris' own mass

[1] Head, Theoretical Mechanics Department, 34 Moskovskoe Shosse; aslanov_vs@mail.ru.

as a thruster fuel source [9]. A promising touchless and low-power solution is the electrostatic tractor [10]. Rigid connection between the space tug and the debris can be realized by a robot arm. The flexible connection can be provided by a tether attached to the space debris. The active debris removal using the space tug with a tether is one of promising techniques [11–14].

The aim of this paper is to provide a simple principle of a reusable, long-term space debris collection system in GEO. The method is based on the use of the unstable libration points L1 or L2 for the two main objects: the Earth and a heavy orbital collector (a moon). The chaser is placed on a line connecting the Earth and the space debris (target), so that the target is located at a small distance from the unstable libration points L1 or L2 towards the chaser. In this configuration the Earth-Target-Chaser system, the target will be attracted to the chaser. For the scope of this paper only in-plane motion of the chaser and the target are considered. If perturbations are absent the target will no longer leave the vicinity of the chaser, bounded by the Hill sphere. As will be shown below, the velocity of the target relative to the chaser is very small, and the task of capturing the target by the chaser.

The importance of the collection and disposal of space debris is determined by the fact that there are 829 objects in GEO, current mass of which is 2359.2 tons. This is almost one third of the total current mass (8144.7 tons) of all objects in near-Earth orbits [15]. The second factor is a collision of objects and a formation of many fragments. There have been four confirmed collision events between catalogued objects so far. One of them is the clash between Iridium 33 and Cosmos-2251 (February 10, 2009) then U.S. space agency NASA estimated that the satellite collision created approximately 1,000 pieces of debris larger than 10 cm, in addition to many smaller ones [16].

The paper discusses only the main idea of the method of capturing space debris based on the use of artificially created libration points. A delivery strategy of the chaser to the place of a moon and transfer space debris to a disposal orbit (which lies to 200-250 km above GEO orbit) are not considered in this paper. The paper consists of four sections and conclusion. In the Section I (Introduction) the research objective is formulated. In Section II the main idea of the proposed method is described and some calculations are given. Section III the motion equations of the system are written in the Local-Vertical-Local-Horizontal frame. In Section IV several numerical examples are considered. Section V investigates the influence of the gravitational pull of the Moon to the motion of the target-chaser system in GEO. At last, the conclusions together with the discussion are drawn in Section VI.

II. Basic Idea of the Method

On the one hand, a lot of space debris is located in GEO, on the other hand, the Earth's gravitational force is much smaller than in LEO. This allows us to pay attention to the restricted three-body problem in the following interpretation. Assume that two point masses m_1 (Earth) and m_2 (chaser), called the primaries revolve around their center mass in circular orbit close to GEO. In the plane of their motion moves a small object (target). Let us answer the question of what should be the mass of the chaser, so that the radius of the Hill sphere is not too small and the velocity of the target in the vicinity of the chaser is not too large.

Here the radius of the Hill sphere is defined as double-distance between Lagrangian points L_1 and (Fig. 1). The Hill radius is given by the well-known formula, see for example [17- 19]

$$r_h \approx r\left(\frac{\mu}{3}\right)^{\frac{1}{3}} \qquad \mu << 1 \tag{1}$$

where $\mu = \frac{m_2}{m_1 + m_2}$, r is the distance between the primaries, m_1 is mass of the Earth, m_2 is mass of the chaser.

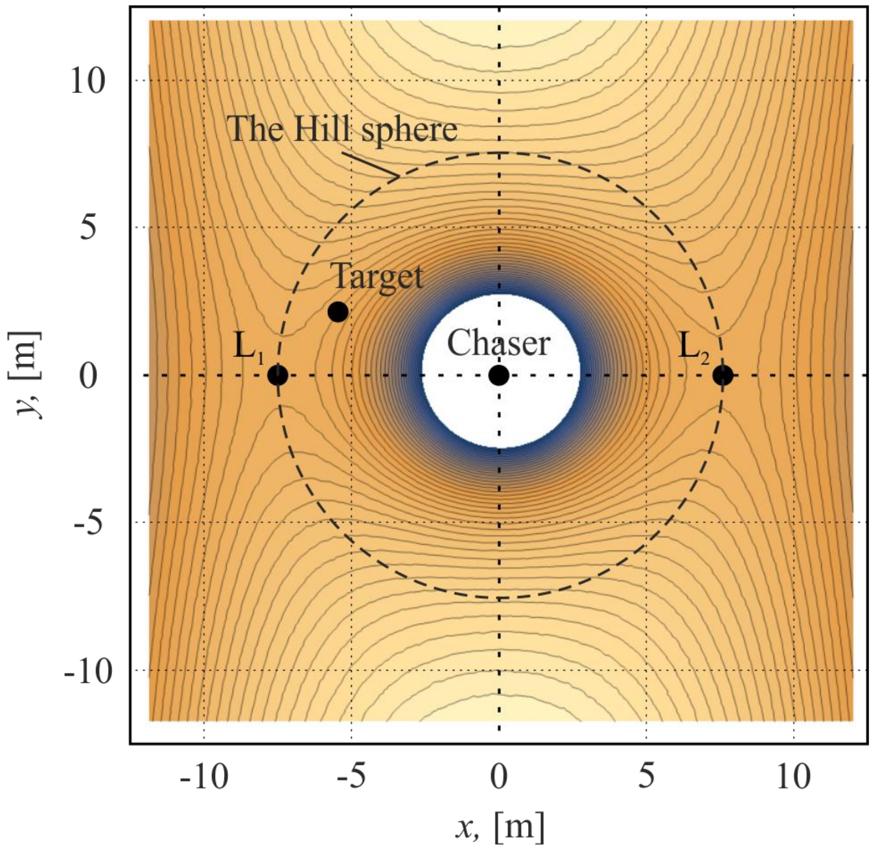

Fig. 1 The Hill sphere and Lagrangian points L_1, L_2

From Table 1 it follows that to capture a small debris it is enough to have the chaser's mass of the order of 10 tons and the chaser's mass should be 100 tons or more for capture a large debris.

Table 1: Radius of the Hill sphere for GEO

Parameter	Value	Value	Value
Mass of the chaser, m_2, kg	10000	100000	1000000
Radius of the Hill sphere r_h, m	3.48	7.48	16.12

The basic idea of the method is to deliver the chaser to place in the configuration of the three-body system (Earth-Chaser-Target), so that the target would be inside the Hill sphere but not including the points L_1 and L_2. In this configuration of the three-body system the target never will leave the area bounded by the Hill sphere. If the velocity of the target relative to the chaser is small, then the target can be easily captured in some vicinity of the chaser using a robot manipulator or other simpler means.

The velocity estimation of the target can be found using the Jacobi integral for a given distance between the chaser and the target. Note that the Jacobi integral is minus twice the total energy per unit mass in the rotating frame of reference: the first term relates to centrifugal potential energy, the second represents gravitational potential and the third is the kinetic energy. The forces that act on the target are the two gravitational attractions, the centrifugal force and the Coriolis force. Since the first three can be derived from potentials and the last one is perpendicular to the trajectory, they are all conservative, so the energy measured in this system of reference is a constant of motion [17-19]

$$J = 2G\left(\frac{m_1}{\sqrt{(x+r\mu)^2+y^2}}+\frac{m_2}{\sqrt{(x-r(1-\mu))^2+y^2}}\right)+n^2(x^2+y^2)-(\dot{x}^2+\dot{y}^2)=const=J_0 \tag{2}$$

where $r = const$ is the distance between the Earth and the chaser, $n = 2\pi / \mathrm{T}$ is the mean motion, x, y are coordinates of the target in the Earth-Chaser frame Oxy (Fig. 2).

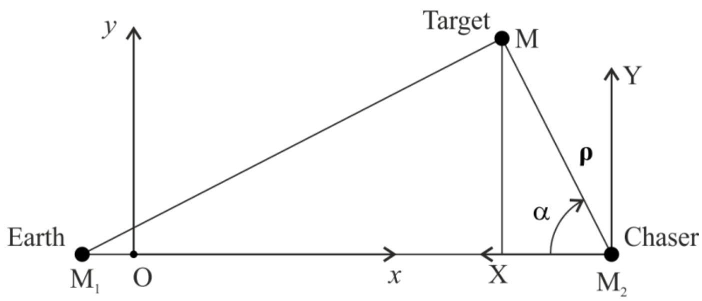

Fig. 2 The Earth-Chaser frame Oxy

One can simply determine the distance between the chaser and the target we use the polar reference frame by a substitution of variables

$$x = (1-\mu)r - \rho\cos\alpha, \quad y = \rho\sin\alpha \tag{3}$$

then the Jacobi integral is written as

$$J = r^2(1-\mu)^2 n^2 - 2r(1-\mu)n^2\rho\cos\alpha + 2G\left(\frac{m_2}{\rho}+\frac{m_1}{\sqrt{r^2-2r\rho\cos\alpha+\rho^2}}\right)+\rho^2(n^2-\dot{\alpha}^2)-\dot{\rho}^2 \tag{4}$$

and

$$J(\rho,\dot{\rho},\alpha,\dot{\alpha}) = const = J_0 \tag{5}$$

Let the trajectory of the target passes through a point that is near the point L_1 inside the Hill sphere

$$\rho_0 = 7.479\,m, \quad \dot{\rho}_0 = 0,\ \alpha_0 = 0,\ \dot{\alpha}_0 = 0 \tag{6}$$

For the chaser mass $m_2 = 100000\ kg$ the Jacobi integral (4) is equal to

$$J_0 = 2.820571515983902 \times 10^7 \frac{m^2}{s^2} \tag{7}$$

Solving (4) and (5) with respect to $\dot{\rho}^2$, can be written

$$\dot{\rho}^2 = -J_0 + r^2 n^2 (\mu - 1)^2 - 2r(\mu - 1) n^2 \rho_1 \cos\alpha_1 + \frac{2Gm_2}{\rho_1} + \frac{2Gm_1}{\sqrt{r^2 - 2r\rho_1 \cos\alpha_1 + \rho_1^2}} + \rho_1^2 \left(n^2 - \dot{\alpha}_1^2 \right) \tag{8}$$

It is obvious that the right-hand side of equation (8) should not be negative and this condition must be satisfied by a pair of values $\alpha_1, \dot{\alpha}_1$. Such the pair for $\rho_1 = 1\,m$ is the following

$$\alpha_1 = 0, \ \ \dot{\alpha}_1 = 0.001\, s^{-1} \tag{9}$$

Finally, formula (8) gives the following the target velocity

$$\dot{\rho} = 0.0031\ m / s \tag{10}$$

Obviously, the target velocity near the chaser is very small, which greatly facilitates the capture of the target.

III. Planar Equations of Motion

To verify the effectiveness of the proposed method of capturing the debris, the planar motion equations of the target relative to the chaser are written in Cartesian coordinates [18, 19]

$$\ddot{x} = \frac{\partial W}{\partial x} + n^2 x + 2n\dot{y}, \qquad \ddot{y} = \frac{\partial W}{\partial y} + n^2 y - 2n\dot{x} \tag{11}$$

where

$$W(x, y) = \frac{Gm_1}{\sqrt{(x + r\mu)^2 + y^2}} + \frac{Gm_2}{\sqrt{(x - r(1 - \mu))^2 + y^2}} \tag{12}$$

Using the substitution of variables (3) the equations (11), (12) are rewritten in the polar coordinates (ρ, α)

$$\ddot{\rho} = r(\mu - 1) n^2 \cos\alpha + \frac{fm_1 (r\cos\alpha - \rho)}{(r^2 - 2r\rho\cos\alpha + \rho^2)^{3/2}} - \frac{fm_2}{\rho^2} + \rho (n - \dot{\alpha})^2, \tag{13}$$

$$\rho\ddot{\alpha} = -fm_1 r \sin\alpha + r(1 - \mu) n^2 \sin\alpha + 2(n - \dot{\alpha})\dot{\rho} \tag{14}$$

We note the first three term in each of the equations (11) can be expressed as the gradient of an effective potential function in Cartesian coordinates [20]

$$V(x, y) = -\frac{2Gm_1}{\sqrt{(x + r\mu)^2 + y^2}} - \frac{2Gm_2}{\sqrt{(x - r(1 - \mu))^2 + y^2}} - n^2 (x^2 + y^2) \tag{15}$$

The last term in the equations (11) are projections of the Coriolis force, therefore the system described by these equations is conservative. The effective potential $V(x,y)$ depends only the coordinates Oxy. So a plot of the effective potential (15) is shown in Fig. 7.4.2 [20] for the Earth-Moon primary system. Here, we will only use a separate fragment of the potential surface to clearly demonstrate the behavior of the target in the vicinity of the chaser (a moon). For this purpose, the effective potential (15) can be written in polar coordinates relative to the chaser by the substitution of variables (3) as

$$V(\rho,\alpha) = -n^2\left(r^2(\mu-1)^2 + \rho^2 + 2r(\mu-1)\rho\cos\alpha\right) - \frac{2Gm_1}{\sqrt{r^2 - 2r\rho\cos\alpha + \rho^2}} - \frac{2Gm_2}{\rho} \tag{16}$$

IV. Numerical Simulation

In this section, using a numerical simulation, we illustrate the main idea of the proposed method. The numerical simulation is based on the numerical integration of the motion equations (13) and (14) for the following initial conditions:

$$\rho_0 = 7.479\,m, \quad \dot{\rho}_0 = 0,\ \alpha_0 = 0,\ \dot{\alpha}_0 = 0,\ t \in \left[0, 2T\right], \tag{17}$$

$$\rho_0 = 5.479\,m, \quad \dot{\rho}_0 = 0,\ \alpha_0 = 0,\ \dot{\alpha}_0 = 0.0001\,s^{-1},\ t \in \left[0, T\right], \tag{18}$$

where T is the orbital period of the chaser around the Earth. We get the chaser mass m_2=100000 kg.

Figs. 3 and 5 show the target trajectories relative to the chaser in the Cartesian coordinates M_2XY (Fig. 2)

$$\boldsymbol{\rho} = \overline{M_2M} = (X,Y) = (\rho\cos\alpha, \rho\sin\alpha) \tag{19}$$

for the initial conditions (17) and (18), respectively.

Figs. 4 and 6 depict the same trajectories on the surface of the reduced effective potential

$$V - V_0$$

where $V_0 = V(r_h, 0)$.

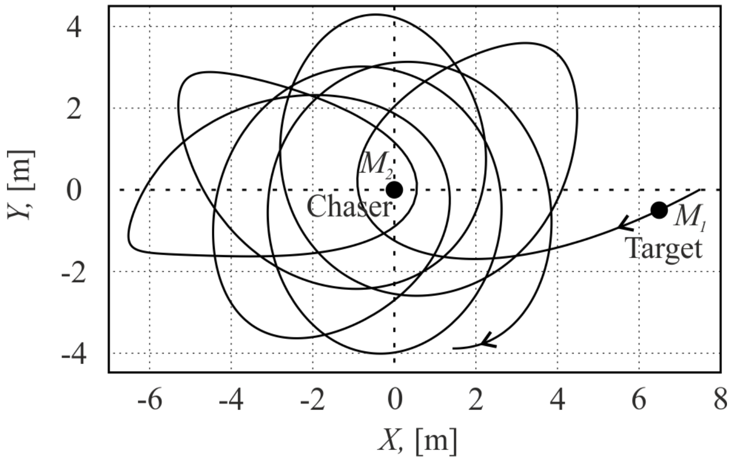

Fig. 3 The target trajectories relative to the chaser in the Cartesian coordinates (19) for the initial conditions (17)

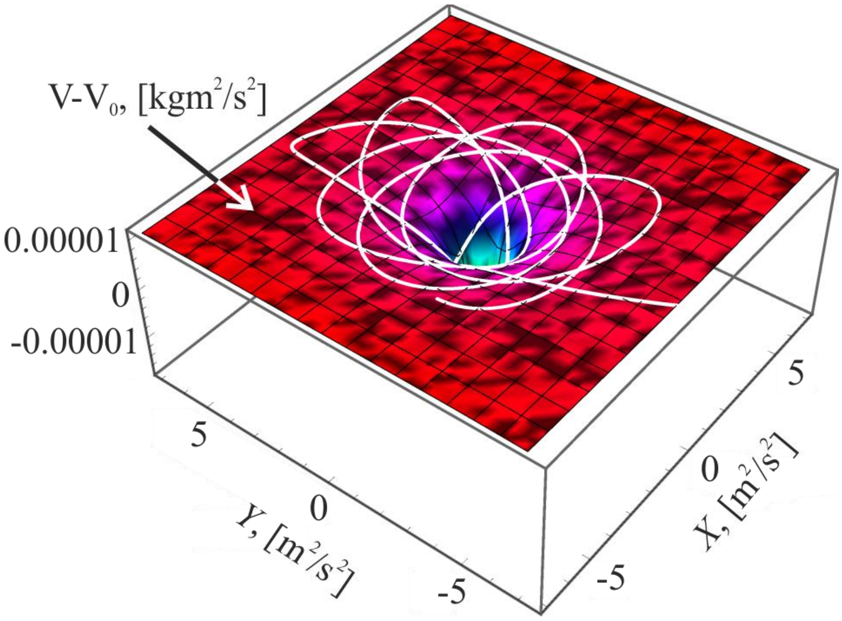

Fig. 4 The target trajectories relative to the chaser in the Cartesian coordinates (19) for the initial conditions (17) on the surface of the reduced effective potential $V - V_0$

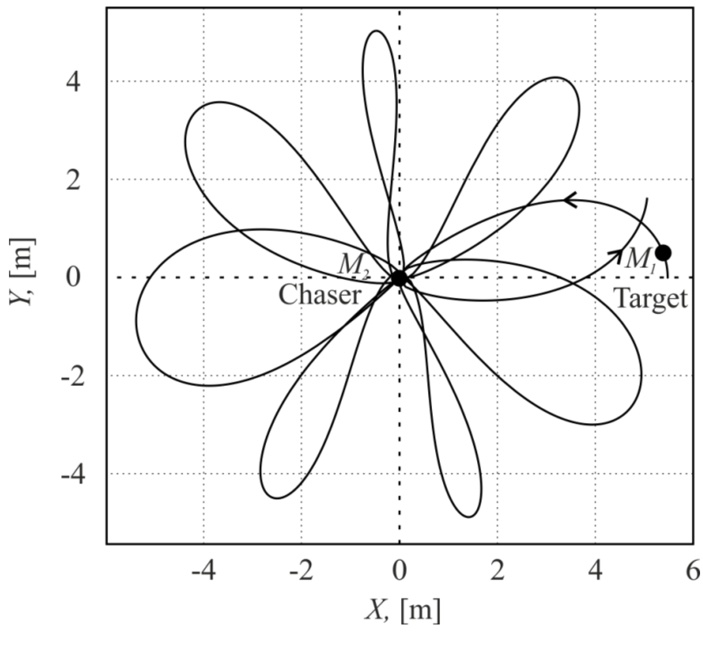

Fig. 5 The target trajectories relative to the chaser in the Cartesian coordinates (19) for the initial conditions (18)

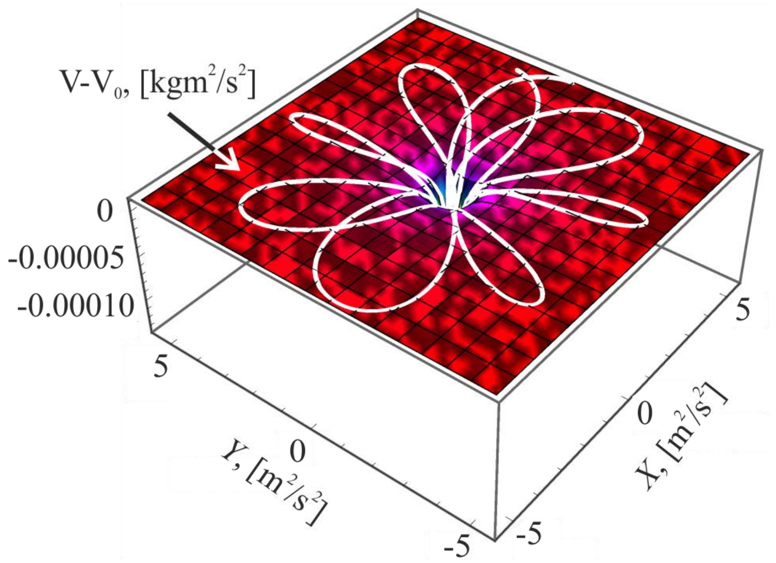

Fig. 6 The target trajectories relative to the chaser in the Cartesian coordinates (19) for the initial conditions (18) on the surface of the reduced effective potential $V - V_0$

In the first case (17), the initial velocity is zero, and in the second case (18) the initial velocity is different from zero. This circumstance has led to that the velocity of the target does not exceed $\left|\dot{\rho}\right| > 0.0021\, m\,/\,s$ in the first case and in the second case $\left|\dot{\rho}\right| > 0.017\, m\,/\,s$.

V. Influence of the Moon to Target and Chaser

This section is devoted to assessing the influence of the gravity of the moon on the relative motion of the target and the chaser. Assuming that the moon's orbit is circular and the motion of the Moon and the chaser with the target occurs in the same plane.

The position of the target relative to the chaser is determined by the vector (19)

$$\boldsymbol{\rho} = \mathbf{r}_1 - \mathbf{r}_2 \tag{20}$$

in the Earth-Moon frame $O_1 x_1 y_1$ vectors $\mathbf{r}_1$ and $\mathbf{r}_2$ are defined as (Fig. 7)

$$\mathbf{r}_2 = \left(x_2, y_2 \right)^T, \ \mathbf{r}_1 = \mathbf{r}_2 + \boldsymbol{\rho} = \begin{pmatrix} x_2 \\ y_2 \end{pmatrix} + \begin{pmatrix} \rho_x \\ \rho_y \end{pmatrix} \tag{21}$$

The motion of the target and the chaser occurs in close halo orbits. The gravitational forces act between the chaser and the target $\mathbf{F}_1 = -\mathbf{F}_2$, which cause corresponding accelerations

$$\mathbf{a}_1 = \frac{\mathbf{F}_1}{m} = \begin{pmatrix} a_{1x} \\ a_{1y} \end{pmatrix} = -\frac{Gm_2}{\rho^3} \boldsymbol{\rho} \tag{22}$$

$$\mathbf{a}_2 = \frac{\mathbf{F}_2}{m_2} = \begin{pmatrix} a_{2x} \\ a_{2y} \end{pmatrix} = \frac{Gm}{\rho^3} \boldsymbol{\rho} \tag{23}$$

In the frame $O_1 x_1 y_1$ the motion equations are written as

$$\ddot{x}_i = \frac{\partial W_i}{\partial x_i} + \omega^2 x_i + 2\omega \dot{y}_i + a_{ix}, \qquad \ddot{y}_i = \frac{\partial W_i}{\partial y_i} + \omega^2 y_i - 2\omega \dot{x}_i + a_{iy} \qquad i = 1,2 \tag{24}$$

$$W_i(x_i, y_i) = \frac{Gm_1}{\sqrt{(x_i + R\mu_m)^2 + y_i^2}} + \delta \frac{Gm_3}{\sqrt{(x_i - R(1-\mu_m))^2 + y_i^2}} \tag{25}$$

where $\mu_m = \dfrac{m_3}{m_1 + m_3}$, m_3 is mass of the Moon, $R = const$ is the distance between the Earth and the Moon, $\omega = 2\pi / \mathrm{T}_m$ is the mean motion the Moon, T_m is the orbital period of the Moon around the Earth.

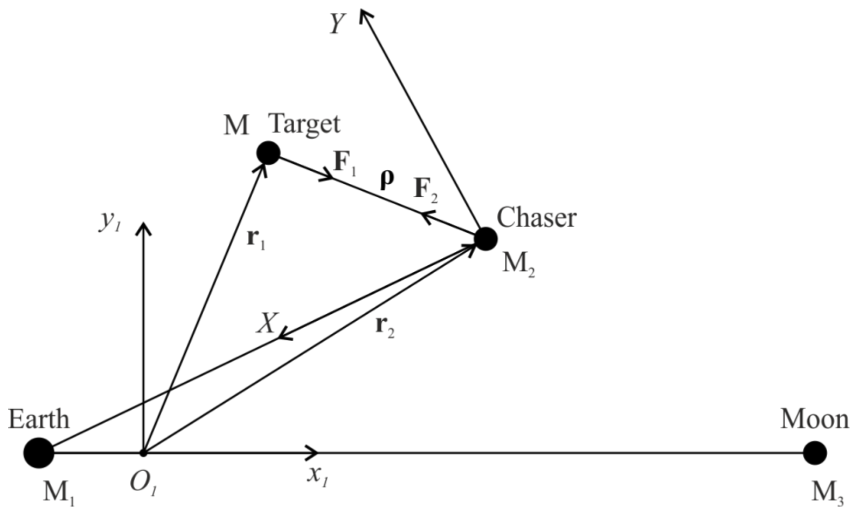

Fig. 7 The Earth-Moon frame $O_1 x_1 y_1$

For $\delta = 1$ the equations (24) describe the motion of the target and the chaser, taking into account the gravitational pull of the Moon, and for $\delta = 0$ without it. Last case was considered above in Sections III and IV. In modeling, the difference in the results of these two cases can show the influence of the gravitational gravitational pull of the Moon on the behavior of the target relative to the chaser.

The numerical simulation is based on the numerical integration of the motion equations (24) for the following initial conditions:

$$\begin{aligned} &x_{20} = 37.49 \times 10^6\, m,\ y_{20} = 0,\ \dot{x}_{20} = 0,\ \dot{y}_{20} = 2.954 \times 10^3\, m/s, \\ &x_{10} = x_{20} - 6\, m, \qquad y_{10} = 0,\ \dot{x}_{10} = 0,\ \dot{y}_{10} = \dot{y}_{20} + 0.0004\, m/s, \end{aligned}, \tag{26}$$

We get the target mass m=1000 kg and the chaser mass m_2=100000 kg. Fig. 7 depicts the target trajectories relative to the chaser in the Cartesian coordinates $M_2 XY$

$$\boldsymbol{\rho} = (X, Y)^T = (\mathbf{e}_X \cdot \boldsymbol{\rho},\ \mathbf{e}_Y \cdot \boldsymbol{\rho})^T \tag{27}$$

where

$$\mathbf{e}_X = -\frac{\mathbf{r}_2 - \mathbf{R}}{|\mathbf{r}_2 - \mathbf{R}|} = \begin{pmatrix} e_{X,x} \\ e_{X,y} \end{pmatrix},\ \ \mathbf{e}_Y = \begin{pmatrix} e_{X,y} \\ -e_{X,x} \end{pmatrix}$$

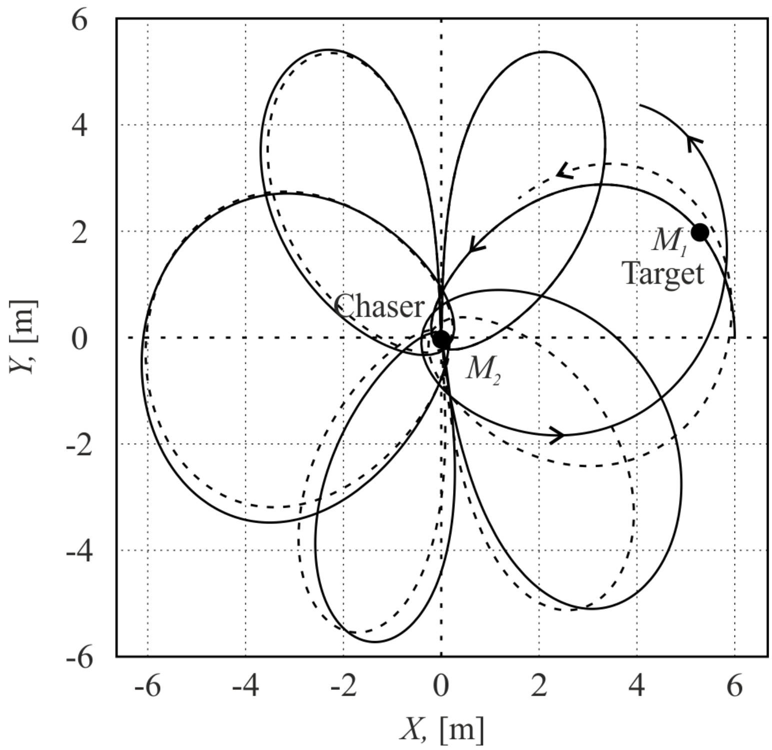

Fig. 8 The target's trajectories relative to the chaser in the Cartesian coordinates (27)

for the initial conditions (26) [solid line- with the Moon, dotted line- without the Moon]

Numerical simulation has shown that the gravity of the moon has little effect on the relative motion of the target-chaser system. This is explained by the fact that the gravity of the moon causes additional acceleration both for the target and for the chaser, and these accelerations are close to each other.

VI. Conclusion

The simple principle of space debris capture was based on the use of the heavy orbital collector placed so that space debris is in an attraction area of the collector confined to the Hill sphere. The basic idea of the proposed method was confirmed by numerical integration of the motion equation of the debris in polar coordinates relative to the collector. To perform gravitational capture of space debris the heavy space collectors (10-100 tons) are required.

The idea of building the heavy orbital collector does not seem more fantastic than building an Earth space elevator that will have a length of about 100 thousand km and a mass of more than 10 thousand tons. Moreover, in the future, the role of the heavy orbital collector can be performed by a relatively small asteroid delivered to GEO.

In the near future the proposed approach can hardly be applied to capture satellites with large solar batteries due to the relatively small radius of the Hill sphere. So if the collector's mass is 100 tons, then the radius of the Hill sphere is equal to 7.48 m (Table 1). However, the capture of small fragments of destroyed satellites may well be realized already now. In this case, the reusable collector of space debris can be useful as a permanent "fire brigade" in GEO.

A few words should be said about different scenarios and problems to be solved for the implementation of the proposed method of collecting and removal of space debris. Two different possible scenarios can be considered. In the first scenario, space debris is first captured in the area bounded by the Hill sphere, and when it hits the area near the collector, and the collector is carried out in a contact manner. The mass of the collector will increase and hence the radius of the Hill sphere will also increase with each absorption of space debris. This can be repeated many times. In the second scenario, space debris will remain within the Hill sphere and will not be captured to inside of the collector. For both scenarios, the common problems are to bring the collector to the desired position in orbit near the debris as shown in Fig. 1, and to study the behavior of the debris within the Hill sphere taking into account perturbations (solar pressure, etc.). In the second scenario there are still separate tasks. First, the transfer of the collector along with the debris to the disposal orbit. Secondly, the debris should be left in disposal orbit and the collector must return to the another debris to repeat its mission. In addition, the collision of debris-collector or debris-debris (a swarm of debris) should also be considered.

In addition, the effect of the gravity of the Moon on the motion of the target relative to the chaser is studied and it is shown that this influence does not change the qualitative picture of the interaction between the target and the chaser.

Perhaps the proposed space debris collection method has great potential to clean of near-Earth space in future missions.

Acknowledgments

This work is supported by the Russian Science Foundation, Project No. 16-19-10158.

References

[1] Bonnal, C., Ruault, J.-M., and Desjean, M.-C., “Active Debris Removal: Recent Progress and Current Trends,” *Acta Astronautica*, Vol. 85, April–May 2013, pp. 51–60. doi:10.1016/j.actaastro.2012.11.009.

[2] Liou, J.-C., Johnson, N., and Hill, N., “Controlling the growth of future LEO debris populations with active debris removal,” *Acta Astronautica*, Vol. 66, No. 5-6, 2010, pp. 648 – 653, doi:10.1016/j.actaastro.2009.08.005.

[3] Kessler, D. J., and Cour-Palais, B. G., “Collision frequency of artificial satellites: The creation of a debris belt,” *Journal of Geophysical Research: Space Physics*, vol. 83, no. A6, pp. 2637–2646, 1978. doi: 10.1029/JA083iA06p02637.

[4] Rui Qi, R., Misra, A. K., and Zuo, Z., "Active Debris Removal Using Double-Tethered Space-Tug System," *Journal of Guidance, Control, and Dynamics*, vol. 40, pp. 722–730, 2013. doi: 10.2514/1.G000699.

[5] Forward, R. L., Hoyt, R. P., and Uphoff, C. W., “Terminator Tether: A Spacecraft Deorbit Device,” *Journal of spacecraft and rockets*, vol. 37, no. 2, pp. 187–196, 2000. doi: 10.2514/2.3565.

[6] Sharf, I., Thomsen, B.,.Botta, B., and Misra, A., “Experiments and simulation of a net closing mechanism for tether-net capture of space debris,” *Acta Astronautica*, vol. 139, no. 7, pp. 332–343, 2017.
doi: 10.1016/j.actaastro.2017.07.026.

[7] S. Kitamura, Y. Hayakawa, and S. Kawamoto, “A reorbiter for large GEO debris objects using ion beam irradiation,” Acta Astronautica, vol. 94, pp. 725–735, Feb. 2014.

[8] Bombardelli, C., and Pelaez, J., “Ion Beam Shepherd for Contactless Space Debris Removal,” *Journal of Guidance, Control, and Dynamics,* vol. 34, no. 3, 2011, pp. 916–920.
doi:10.2514/1.51832.

[9] Kumar, R., and Sedwick, R. J., “Despinning Orbital Debris Before Docking Using Laser Ablation,” *Journal of Spacecraft and Rockets*, vol. 52, no. 4, 2015, pp. 1129–1134.
doi:10.2514/1.A33183.

[10] Schaub, H., and Moorer, D. F., “Geosynchronous Large Debris Reorbiter: Challenges and Prospects,” *The Journal of the Astronautical Sciences*, Vol. 59, No. 1–2, 2014, pp. 161–176.
doi:10.1007/s40295-013- 0011-8.

[11] Cougnet, C., Alary, D., Gerber, D., Utzmann, J., and Wagner, A., “The debritor: an "off the shelf" based multimission vehicle for large space debris removal,” 63rd International Astronautical Congress, pp. 1–6, 2012.

[12] Jasper, L., and Schaub, H., “Input shaped large thrust maneuver with a tethered debris object,” *Acta Astronautica*, vol. 96, pp. 128–137, Mar. 2014.
doi:10.1016/j.actaastro.2013.11.005.

[13] Aslanov, V., and Yudintsev,V., “Dynamics of Large Debris Connected to Space Tug by a Tether,” *Journal of Guidance, Control, and Dynamics*, vol. 36, no. 6, pp. 1654–1660, 2013.
doi: 10.2514/1.60976.

[14] Aslanov, V., and Yudintsev,V., “Behaviour of tethered debris with flexible appendages,” *Acta Astronautica*, vol. 104, pp. 91–98, July 2014.
doi: 10.1016/j.actaastro.2014.07.028.

[15] ESA’s Annual Space Environment Report, Technical Note, 18 May 2018.
https://discosweb.esoc.esa.int/web/guest/statistics.

[16] Oleksyn., V., "What a mess! Experts ponder space junk problem". *Associated Press*. Retrieved 20 May 2010.

[17] Koon, W., Lo, M., Marsden, J., and Ross, S., *Dynamical Systems, the Three-Body Problem and Space Mission Design*, Interdisciplinary Applied Mathematics (48) Springe,r New York, pp.400, 2017.

[18] Schaub, H., and Junkins, J., *Analytical Mechanics of Space Systems,* AIAA Education Series, 2nd Edition, Reston, VA, 2009.
doi:10.2514/4.867231.

[19] Szebehely, V., *Theory of Orbits: The Restricted Three Body Problem,* Academic Press San Diego, 1967.

[20] Fowles, G.R., and Cassidy, G.L., Analytical Mechanics, 7th ed. Thomson, 2004.
http://physics.princeton.edu/~mcdonald/examples/mechanics/fowles_mechanics_04_pp312-321.pdf